Unravelling the mechanism of peptide nanofibril fluorescence

Luka Skoric

May 2017

PIs: Dr Gabriele Kaminski Schierle, Dr Dan Credington
Daily supervisors: Dr Amberley Stephens, Saul Jones

Declaration: "This report is substantially my own work and conforms to the University of Cambridge's guidelines on plagiarism. Where reference has been made to other research or work done by me in collaboration with others, this is clearly acknowledged in the text, bibliography and acknowledgements."

Abstract

Amyloid protein fibrils have been shown to absorb light in the near UV range and exhibit intrinsic fluorescence in the visible range. The mechanism behind this phenomenon is not well understood as it is exists even in the absence of aromatic amino acids that characterise conventional protein fluorescence. Recent simulations point to the importance of proton transfer across hydrogen bonds between individual fibril structures in the mechanism of the fluorescence. In this project, we further investigate fibrilisation and the optical properties of amyloid-β fibrils and correlate them with the simulations. The fibrilisation of $A\beta_{30-35}$ at pH 7.4 and $A\beta_{1-42}$ at both low and high pH is demonstrated. Moreover, we show that $A\beta_{30-35}$ has a similar absorption characteristic to $A\beta_{1-42}$ and displays intrinsic fluorescence in the range 330-380 nm under 290 nm light

1 Introduction

The failure of proteins to fold correctly, or to remain correctly folded, is the origin of a wide variety of pathological conditions including neurodegenerative diseases such as Alzheimer's (AD) and Parkinson's disease (PD) which affect millions of people worldwide [1]. AD is characterised by peptide fragments amyloid-β and tau proteins which form insoluble and highly ordered linear deposits in the brain of these patients, known as amyloid fibrils. Understanding the mechanisms of fibril formation, the kinetic aspects of their aggregation and, more recently, their optical properties are areas of active research and are seminal for the understanding of the development of neurodegenrative diseases [2].

Even though the morphology, size and function of parent polypeptides can be remarkably diverse, all amyloid fibres share common structural properties. They consist of stacks of highly ordered β-strands that lie perpendicular to the fibril central axis and are connected by hydrogen bonds in a so-called cross-β arrangement [3] [4]. It is thought that this network of hydrogen bonds is responsible for the remarkable thermodynamic stability [5], mechanical strength and stiffness of amyloid fibrils [6]. These properties are the reason for their persistance in biological systems once the fibrils are formed. Moreover, recently a link has been found between the amyloid structures and the intrinsic fluorescence phenomenon in the visible range [7–9].

Multiple recent studies have shown that protein fibrils absorb light at wavelengths $\lambda > 360$ nm and have a red-shifted fluorescence at $\lambda > 400$ nm with lifetimes of 1-3 ns [7, 9, 10]. It has been proposed that this intrinsic fluorescence could be used as a label-free, quantitative assay of amyloid fibril growth which could further the study of protein aggregation and the search for potential therapeutic compounds [11]. The mechanism behind this process is still under investigation. Most organic compounds use delocalised electrons in sequences of alternating single and multiple bonds, known as conjugated systems, to absorb light and fluoresce. However, recent evidence has shown that protein fibrils exhibit similar characteristic fluorescence even when the aromatic amino acids containing conjugated bonds have been removed [7, 10, 11].

The role of hydrogen bond networks in determining the optical properties of β-rich biological systems has been investigated since the 1950s [12]. Several studies have proved, both through computational models and experimental procedures, that the displacement of protons along the interaction axis, such

as hydrogen bonds, can strongly affect the photophysics of organic molecules [10, 13, 14]. Hence, it has been hypothesised that the proton delocalization in the extensive hydrogen bond network between amyloid fibres is responsible for the observed fluorescence phenomenon [10].

In their recent paper, Pinotsi *et al.* [10] from the Cambridge Molecular Neuroscience Group (MNG) used time-dependent density functional theory (TD-DFT) and molecular dynamics simulation (MDS) to demonstrate that "specific H-bonds in protein fibrils are permissive to proton transfer, leading to situations in which the proton can be found on either the N- or the C-terminus and thus to the creation of a double well ground state potential that is likely to have a consequence on both the absorption and emission characteristics of the system". Due to computational complexity, the simulations were performed on crystal structures of short fragments of amyloid β proteins. Moreover, they compared the excitation emission spectra of the intrinsic fluorescence of the aromatic residue-containing, human $A\beta_{1-42}$ and aromatic residue-free $A\beta_{33-42}$. They found that the spectra of both fibrils are largely the same with peaks of emission and excitation at 450 nm and 350 nm respectively.

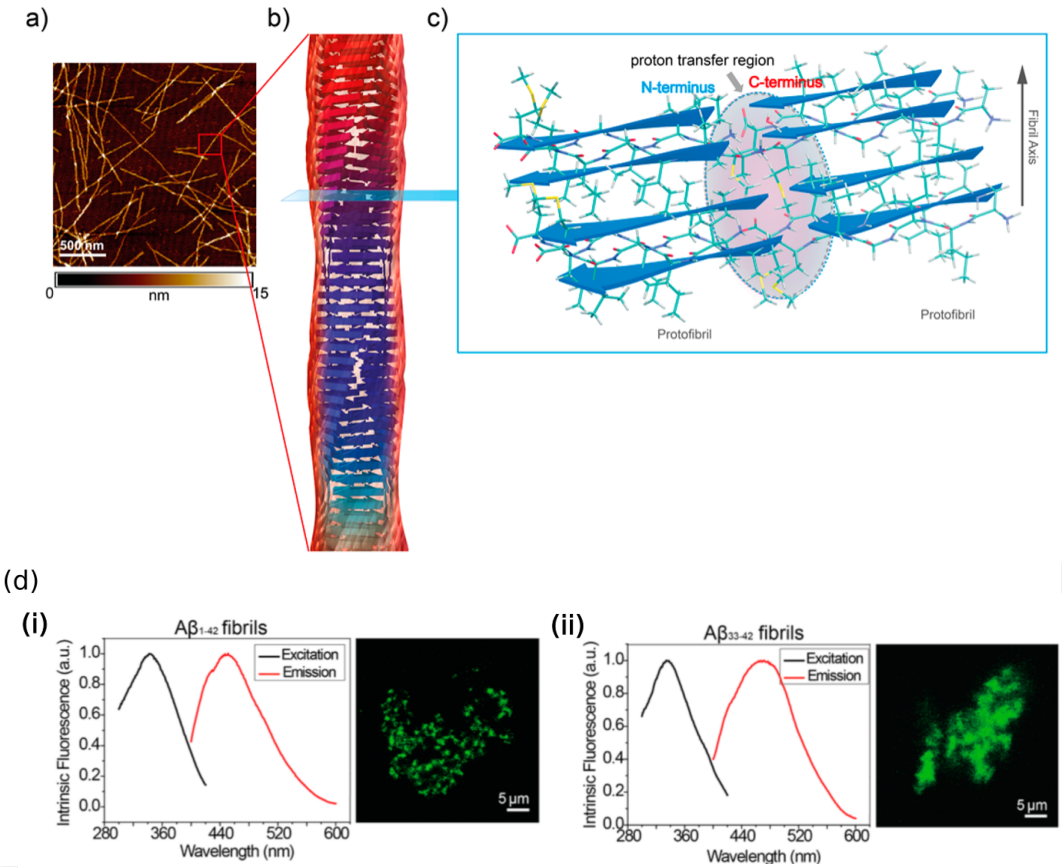

Figure 1: Adapted from Pintosi *et al.* [10]. Structure of a protein fibril: (a) Atomic force microscopy of protein fibrils, (b) schematic view of the 3D peptide arrangement in a protein fibril consisting of four filaments twisted around the same axis, (c) magnified cross-section showing stacks of β-strands from two adjacent peptide chains and the region where proton transfer is thought to occur. of (i) $A\beta_{30-35}$ and (ii) $A\beta_{30-35}$ with emission centered at 450 nm and excitation at 365 nm.

One of the goals of the MNG group is to further investigate the proton delocalisation hypothesis. The aim of this project was to compare the optical properties of amyloid-β fibril samples and correlate them with the results of DFT simulations. The monomers used to grow fibrils correspond to: the full length synthetic analogue of human $A\beta_{1-42}$; one of the aromatic residue-free fragments $A\beta_{30-35}$ on which DFT simulations were performed; and the version of the latter with acetylated N-termini (Figure 2).

If the proton delocalisation, as opposed to conjugated bonds, is the main driver of the fluorescence, we expect $A\beta_{1-42}$ and $A\beta_{30-35}$ to have a similar fluorescence signature. As the simulations show that the highest proton delocalisation occurs between C and N termini of protofibrils, the acetylated protein should have a significantly quenched signal due to the acetyl group interfering with the hydrogen bonding. However, it was expected that the hydrogen bond

network between individual monomers should remain unaffected, allowing for the fibril formation.

Moreover, the samples of $A\beta_{1-42}$ in different pH were prepared and tested for fibrilisation. It is expected that fully protonating or deprotonating the fibrils at pH = 0 or 14 respectively, will have a significant impact on their optical properties [10], but further measurements were outside the scope of this project. In this project, I firstly investigated the fibrilisation of the samples from the monomers, secondly measured the absorption of the samples and finally, measured the excitation and emission spectra of the intrinsic fluorescence of the amyloid peptide samples. I then compared these data with the results acquired by Pinotsi *et al.*in their previous paper.

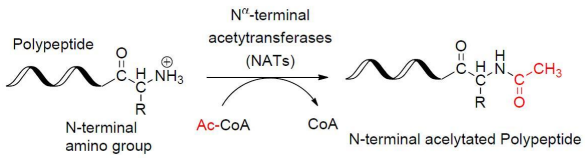

Figure 2: Actylation of N-termini of a polypeptide chain

2 Experimental section

2.1 Sample preparation

Phosphate-buffered saline (PBS) buffer was prepared by dissolving 1 PBS tablet from OXoid in 100 mL water. Appropriate amount of HCl or NaOH was added to adjust the pH to the required value. All buffers were made with Milli-Q water and were further filtered before use. Lyophilized $A\beta_{1-42}$, $A\beta_{30-35}$ and acetylated $A\beta_{30-35}$ peptides were dissolved in PBS of pH 7.4 in Eppendorf tubes. $A\beta_{1-42}$ was further split into three samples which were diluted with PBS of pH = 0, 7.4 and 14 in the ratio 1:3.5. The final concentration of the three different pH values of $A\beta_{1-42}$ was 100 μM while the two remaining samples were prepared in 600 μM concentrations. We used a higher concentration of the two $A\beta_{30-35}$ samples as their tendency for fibrilisation is expected to be lower.

The solutions were incubated for 7 days at 37°C to ensure that there was sufficient time for the consumption of monomeric protein and conversion to fibrils. After incubations, the solutions were kept at 5° in Eppendorf tubes to ensure the stability between measurements.

2.2 Confocal microscopy

To look for signs of fibrilisation and fluorescence, we observed the samples in fluid under confocal microscopy. The sample was excited with a 405 nm wavelength laser and the detector set to be integrating the emission in the range 425-500 nm. However, the confocal measurements were only qualitative as the set-up did not have a 405 nm filter, meaning that the artefacts from scattering were possible.

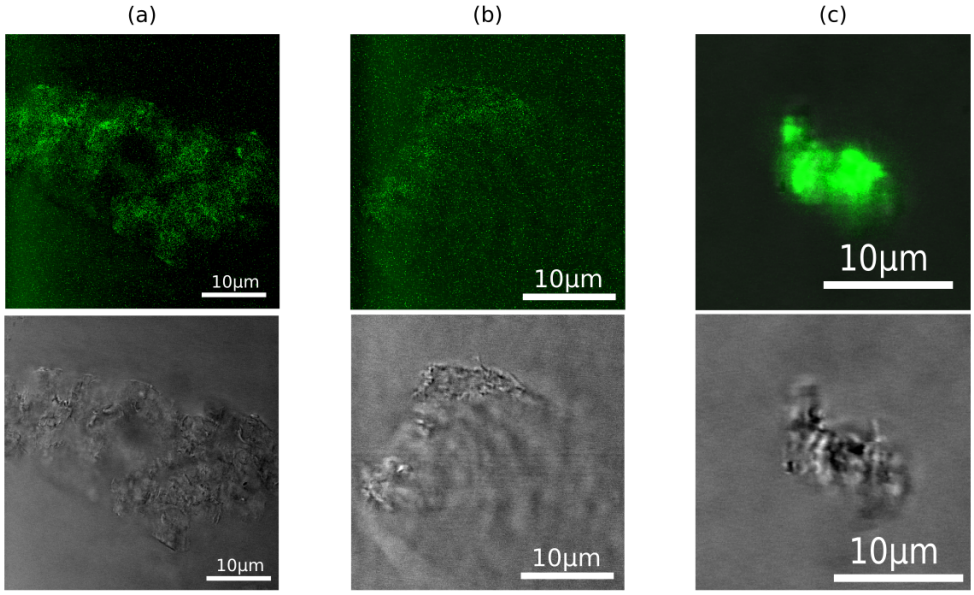

Figure 3: Confocal microscopy images of amyloid peptides. Fluorescence (top) and differential interference contrast microscopy (DIC) (bottom) under 405 nm excitation of: (a) $A\beta_{1-42}$, (b) $A\beta_{30-35}$, (c) acetylated $A\beta_{30-35}$.

The laser wavelenegth is likely not optimal for the samples as $A\beta_{1-42}$ is expected to have the excitation peak around 350 nm [10]. Nevertheless, bleaching-prone weak fluorescence could be seen (Figure 3) and suggests the existence of fibrils in $A\beta_{1-42}$ and $A\beta_{30-35}$. The acetlyated sample showed much brighter, well-defined spots which were resistant to bleaching and had no visible fibril structures. Since these could be the artefact of strong scattering, further investigation was required.

2.3 Atomic Force Microscopy

The amyloid fibrils were deposited on mica and imaged in air under atomic force microscopy (AFM). The samples were prepared by incubating 20 μL of the respective solution for 1 hour, followed by washing with Milli-Q water to remove any leftover PBS crystals. The Bruker's Bioscope Resolve AFM was operated under PeakForce Tapping mode with Scanasyst-Air tips of 2 nm radii.

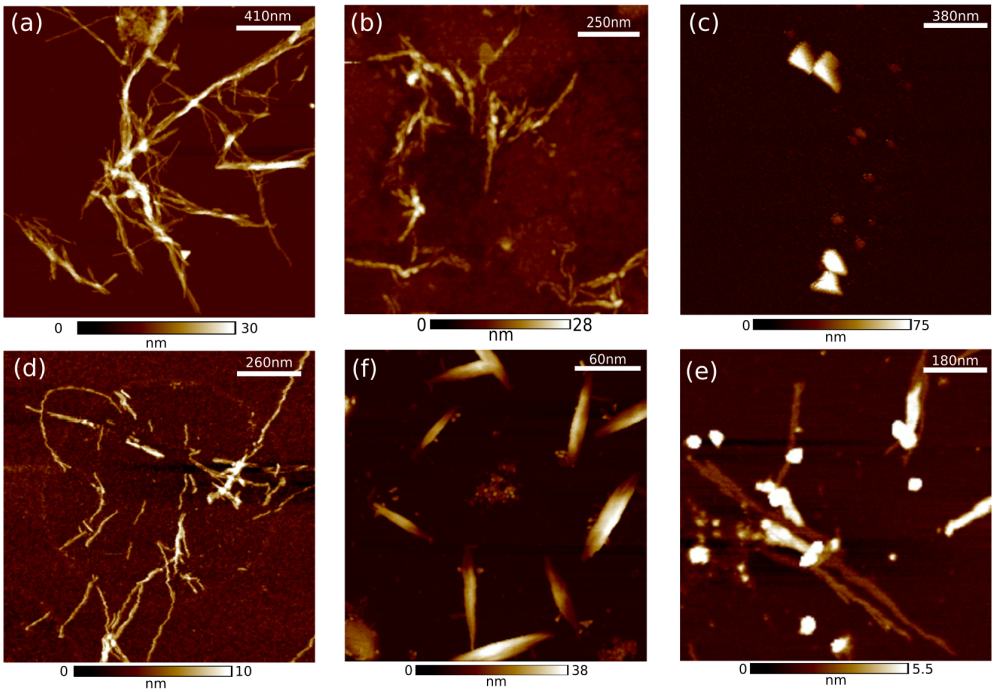

Figure 4: Atomic Force images of amyloid proteins in PeakForce tapping mode. Samples grown at pH7.4: (a) $A\beta_{1-42}$, (b) $A\beta_{30-35}$, (c) acetylated $A\beta_{30-35}$. Samples of $A\beta_{1-42}$ grown at (d) low pH and (e),(f) high pH

From the AFM images (Figure 4), we can see that all samples, apart from the acetylated $A\beta_{30-35}$, have fibrilised . The high pH $A\beta_{1-42}$ had short fibrils and thicker, elongated structures out which individual fibrils seemed to grow (Figure 4). Moreover, there looks to be a higher tendency to form bundles of fibrils the higher the pH is. This behaviour is unusual and warrants further investigation.

Acetylated samples formed well defined crystals instead of fibrils (Figure 4c). Since the acetylation only affects the N-termini of monomers, it was expected that the hydrogen bond network between β-sheet layers will remain largely intact and the fibrils similar to the non-acetylated samples (Figure 4b) will form. However, two different batches of acetylated sample were prepared and neither of them showed fibril structures under AFM. It has been recorded that $A\beta_{30-35}$ forms microcrystals, even under fibrilisation conditions, and fibres can grow from the tip of the microcrystal [15]. Hence, it could be the case that acetylation changes the structure in a way that favours crystals, preventing the formation of fibril structures.

2.4 Optical properties

We measured the optical properties of the samples in PBS buffer with pH 7.4. The integrating sphere UV-vis spectrophotometer was used to acquire the absorption data with the sample in 1 mm path-length quartz cuvette (Hellma Analytics). This method was chosen as it subtracts the majority of scattering

artefacts and is sensitive enough to detect the low absorbing features of our samples.

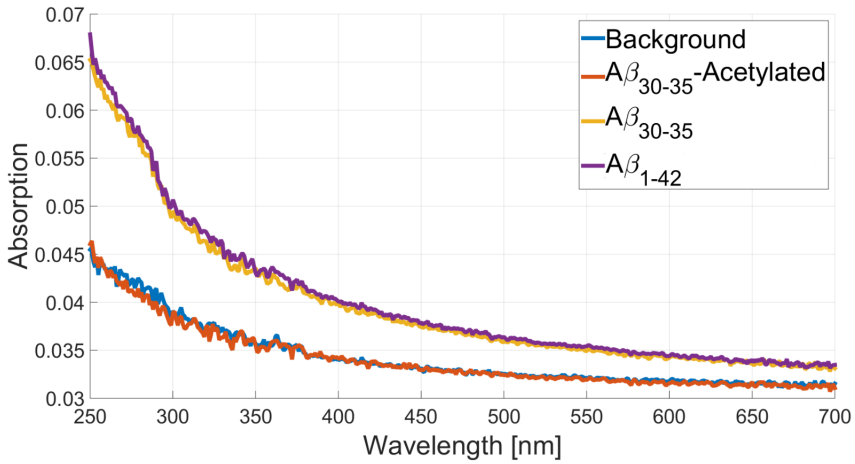

Figure 5: Absorption spectra of $A\beta_{1-42}$, $A\beta_{30-35}$ and acetylated $A\beta_{30-35}$ compared to pH 7.4 buffer background

Due to the low absorbance and fluorescence intensity, to get a measurable emission signal, we needed to maximise the optical density of our samples. Initial measurements showed that the direct fluorescence measurements of the prepared solutions makes them hard to distinguish from the background. Hence, we centrifuged 2 tubes with 300μL each for both $A\beta_{30-35}$ and acetylated $A\beta_{30-35}$ at 21,100g for 20 minutes and collected 25μL pellets. Same procedure was applied to $A\beta_{1-42}$, but the starting volumes were 100μL. The collected pellets were then measured in fluorescence spectrophotometer (Hitachi F-4500) using 3×3 mm path length quartz cuvettes (Hellma Analytics). This procedure allows us to significantly increase the optical density of our solutions, but at the expense of the precise control over sample concentrations.

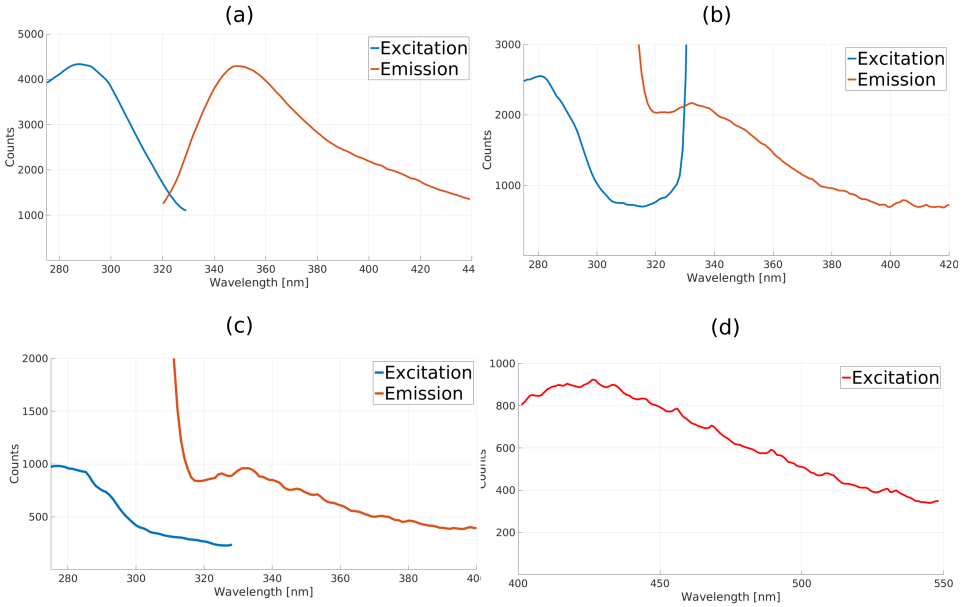

Figure 6: Emission and excitation spectra of the intrinsic fluorescence of amyloid protein solutions: (a),(b) $A\beta_{30-35}$, (c) acetylated $A\beta_{30-35}$, (d) $A\beta_{1-42}$. In (a), (b) and (c) excitation spectra, the emission was centred at 350 nm, and for the emission spectra the excitation was centred at 290 nm. For $A\beta_{1-42}$ (d), the exitation was centered at 340 nm in order to replicate the conditions from [10]. The extremely steep peaks in (b) and (c) are the artefacts of the emission and excitation windows overlapping

From the integrating sphere measurements, we can see that the acetylated sample does not have any significant absorption above the background buffer. Moreover, $A\beta_{1-42}$ and $A\beta_{30-35}$ have a surprisingly similar absorption feature with a change in the gradient at about 280 nm. The samples absorb very weakly, with peak absorption being only 6.5% at 250 nm. However, the distinction between the background and $A\beta_{1-42}$ and $A\beta_{30-35}$ is well within the error of the measurement apparatus. DFT simulations from Pinotsi *et al.*have shown a similar gradient change at ∼260 nm transition. However, only a qualitative comparison can be made since the simulations were done with model systems at 0K and do not include a high degree of scattering in real fibrillar materials.

The acetylated sample has shown a sign of a peak in emission at 330 nm (Figure 6c). However, the intensity is very low and could be the consequence of a small level of cross contamination, even though all measures were taken to avoid it. Due to no noticeable absorption and lack of fibrilisation, we would not expect the acetylated sample to fluoresce.

$A\beta_{1-42}$ shows a very weak peak in emission at 440 nm when excited by 340 nm light (Figure 6d). This is close to 450 nm peak found by Pinots *et al.*(Figure 1d). A blank PBS buffer was shown to have between 200 and 400 photon counts throughout the spectrum under the same conditions. Hence, the measured fluorescence could have been affected by the PBS background resulting in a peak 10 nm different than the one observed in literature.

The excitation and emission scans of $A\beta_{30-35}$ were measured to have peaks

at 290 nm and 350 nm respectively (Figure 6a). The subsequent measurements on a different batch have shown a slightly blue shifted features with peaks at 280 nm and 335 nm respectively, but with a much lower brightness. The difference in brightness is likely due to different fibril concentrations. Nevertheless, it is apparent that $A\beta_{30-35}$ has an intrinsic fluorescence which is excited by 285 nm light and emits in 330-380 nm range.

3 Conclusion and further work

We demonstrated that $A\beta_{30-35}$ forms fibril structures when incubated in PBS (pH 7.4) for 7 days. $A\beta_{1-42}$ forms fibrils at all pH with a higher tendency to form bundles of fibrils at basic conditions. Moreover, we have shown that acetylation of $A\beta_{30-35}$ affects the properties of the peptide in a way that prevents fibrilisation under the applied growing conditions.

The $A\beta_{30-35}$ displays the absorption characteristic very similar to the full length human $A\beta_{1-42}$. In addition, an intrinsic fluorescence in the range 330-380 nm under 290 nm light was detected, despite the lack of conjugated bonds. These findings support the proton delocalisation hypothesis. However, the excitation and emission are both blue shifted when compared to $A\beta_{1-42}$ indicating some distinction in the florescence mechanism which should be further investigated. The acetylated sample showed a significantly reduced fluorescence. However, since it does not form fibrils, the optical properties cannot easily be related to the proton delocalisation hypothesis.

The Molecular Neuroscience Group plans to continue researching the mechanism behind intrinsic fluorescence of $A\beta_{1-42}$ and other amyloid proteins. In collaboration with Italy, FTIR measurements on $A\beta_{1-42}$ and $A\beta_{30-35}$ samples are planned. Furthermore, these findings should be repeated with higher optical densities, allowing for more precise data collection. Since water quenches some of the fluorescence, one of the proposed ways of achieving a higher brightness is to dry the solutions on quartz slides and measure with a high intensity excitation source. Moreover, it would be interesting to see fibrils under scanning near-field optical microscopy (SNOM) which would allow for direct correlation between the intrinsic fluorescence and the structural arrangement. However, this is challenging due to low wavelengths required for excitation of amyloid fibrils.

References

[1] Christopher M. Dobson. Protein folding and misfolding. *Nature*, 426, December 2003.

[2] Dr Gabriele S. Kaminski Schierle *et al.*. A fret sensor for non-invasive imaging of amyloid formation in vivo. *ChemPhysChem*, 12(3):673–680, February 2011.

[3] Anthony W. P. Fitzpatrick *et al.*. Atomic structure and hierarchical assembly of a cross-β amyloid fibril. *PNAS*, 110(14):5468–5473, April 2013.

[4] Thomas R. Jahn *et al.*. The common architecture of cross-β amyloid. *J. Mol. Biol.*, 395:717–727, 2010.

[5] Andrew J. Baldwin *et al.*. Metastability of native protein and the phenomenon of amyloid formation. *JACS*, 2011.

[6] Tuomas P. J. Knowles *et al.*Jeffrey F. Smith. Characterization of the nanoscale properties of individual amyloid fibrils. *PNAS*, 103(43):15806–15811, October 2006.

[7] Anshuman Shukla, Sourav Mukherjee, Swati Sharma, Vishal Agrawal, K.V. Radha Kishan, and P. Guptasarma. A novel uv laser-induced visible blue radiation from protein crystals and aggregates: scattering artifacts or fluorescence transitions of peptide electrons delocalized through hydrogen bonding? *Arch. Biochem. Biophys.*, 428:144–153, 2004.

[8] Loretta Laureana del Mercato *et al.*. Charge transport and intrinsic fluorescence in amyloid-like fibrils. *PNAS*, 104(46):18019–18024, November 2007.

[9] Fiona T. S. Chan, Gabriele S. Kaminski Schierle, Janet R. Kumita, Carlos W. Bertoncini, Christopher M. Dobson, and Clemens F. Kaminski. Protein amyloids develop an intrinsic fluorescence signature during aggregation. *Analyst*, 138:2156–2162, 2013.

[10] Dorothea Pinotsi, Luca Grisanti, Pierre Mahou, Ralph Gebauer, Clemens F. Kaminski, Ali Hassanali, and Gabriele S. Kaminski Schierle. Proton transfer and structure-specific fluorescence in hydrogen bond-rich protein structures. *J. Am. Chem. Soc.*, 138:3046–3057, 2016.

[11] Dorothea Pinotsi, Alexander K. Buell, Christopher M. Dobson, Gabriele S. Kaminski Schierle, and Clemens F. Kaminski. A label-free, quantitative assay of amyloid fibril growth based on intrinsic fluorescence. *ChemBioChem*, 14:846–850, 2013.

[12] E. Schauenstein and G.Z. Perko. *Der. Bunsengesellschaf Phys.Chem.*, 57(927-934), 1953.

[13] Luke M. Oltrogge, Quan Wang, and Steven G. Boxer. Ground-state proton transfer kinetics in green fluorescent protein. *Biochemistry*, 53:5947–5957, 2014.

[14] A. L. Sobolewski, W. Domcke, C. Dedonder-Lardeuxc, and C. Jouvetc. Excited-state hydrogen detachment and hydrogen transfer driven by repulsive $\pi\sigma^*$ states: A new paradigm for nonradiative decay in aromatic biomolecules. *Phys. Chem. Chem. Phys.*, 4:1093–1100, 2002.

[15] Jacques-Philippe Colletier *et al.*. Molecular basis for amyloid-βpolymorphism. *PNAS*, 108(41):16938–16943, October 2011.